# Contribution of Climate Change and Urbanization to the Variation of Extreme Precipitation in the Urban Agglomerations over the Loess Plateau

Na Wei[1], Ninglian Wang[1], and Yu rong zheng[2]

[1]Northwest University
[2]North-West University

September 25, 2021

**Abstract**

With global warming and rapid urbanization, urban agglomerations over the Loess Plateau (LP) are suffering from various urban disasters. Urbanization has aggravated the decreasing trends of extreme precipitation in Taiyuan and Xi'an urban agglomerations (UAs) and enhanced the increasing trends of extreme precipitation in Luoyang, Hohhot and Xining UAs during 1979–2018. Meanwhile, the number of light rain days decreases in almost all the cities, indicating the sensitivity of light rain days to urbanization. The climate change is a primary contributor to the change of urban precipitation during 1980–2000. However, the urbanization contribution has been increasing gradually since 2000, and the urbanization further amplifies the trend of extreme precipitation caused by the climate change. In terms of the physical mechanisms, the rapid increasing surface temperature and aerosol particles are closely related to the urban precipitation. Our findings provide a systematic understanding of the urbanization effects on the extreme precipitation over the LP and may play an important role in the mitigation of urban disasters.

Contribution of Climate Change and Urbanization to the Variation of Extreme Precipitation in the Urban Agglomerations over the Loess Plateau

Na Wei[1,2], NinglianWang[1*], Yurong Zheng[1]

[1]Shaanxi Key Laboratory of Earth Surface System and Environmental Carrying Capacity, Northwest University, Xi'an, Shaanxi Province, China, 710027

[2] Climate Centre of Shaanxi Province, Xi'an, China, 710049

**Abstract:** With global warming and rapid urbanization, urban agglomerations over the Loess Plateau (LP) are suffering from various urban disasters. Urbanization has aggravated the decreasing trends of extreme precipitation in Taiyuan and Xi'an urban agglomerations (UAs) and enhanced the increasing trends of extreme precipitation in Luoyang, Hohhot and Xining UAs during 1979–2018. Meanwhile, the number of light rain days decreases in almost all the cities, indicating the sensitivity of light rain days to urbanization. The climate change is a primary contributor to the change of urban precipitation during 1980–2000. However, the urbanization contribution has been increasing gradually since 2000, and the urbanization further amplifies the trend of extreme precipitation caused by the climate change. In terms of the physical mechanisms, the rapid increasing surface temperature and aerosol particles are closely related to the urban precipitation. Our findings provide a systematic understanding of the urbanization effects on the extreme precipitation over the LP and may play an important role in the mitigation of urban disasters.

Key words: Urban Extreme Precipitation Climate Change Urban Heat Island

## Introduction

Global warming and urbanization are both rapidly changing the urban climate environment, causing a series of urban climate problems, such as urban heat island (UHI), urban waterlogging and water shortage, and air pollution (Della-Marta, Haylock et al. 2007, Han, Baik et al. 2014, Ma, Li et al. 2018, Paul, Ghosh et al. 2018). The UHI has been a common phenomenon resulted from the urbanization, but it demonstrates different impacts on the precipitation under different climatic backgrounds (Wang, Zhou et al. 2007, Daniel, Lemonsu et al. 2018, Ma, Li et al. 2018, Yan, Chan et al. 2020, Yang 2020){Chrysanthou, 2014 #30;Mazdiyasni, 2015 #23}. Many studies revealed that the UHI can induce updrafts and trigger moist convections, resulting in more frequent extreme precipitation near the urban areas, such as Beijing and the Pearl River Delta, than in the rural areas (Della-Marta, Haylock et al. 2007, Drobinski, Silva et al. 2016). In the urban agglomerations (UAs) of the Yangtze River Delta in East China, there is a prominent urban dry island (UDI) effect, which is characterized by reduced humidity and increased vapor pressure deficit in the urban core area (Du, Wang et al. 2019, Luo and Lau 2019). Some researchers concluded that the urbanization tends to augment the precipitation trends caused by the climate change at national scale in China (Gu, Zhang et al. 2019). Moreover, the UHI effects are enhanced more obviously in wet climates than in dry climates (Zhao, Lee et al. 2014). It can be found that the urbanization impact on temperature and precipitation may also be different under different climatic backgrounds and terrain conditions (Liao, Liu et al. 2018). Climate change is a dominant contributor for the urban precipitation trends, but the urbanization has been exhibiting a relatively strong influence since the reform and opening up in China. Assessing the contributions of climate change and urbanization to the changes in urban precipitation is important for the disaster risk management.

Previous studies mainly evaluated the urbanization effect by analyzing the difference between urban and rural meteorological observation stations (Zhao and Wu 2017, Luo and Lau 2018, Ma, Li et al. 2018). Because of the urban expansion, the distance between urban and rural stations and the number of urban and rural stations vary greatly, which may cause uncertainty of the urbanization effect evaluation (Song, Zhang et al. 2014). High-resolution gridded precipitation data and artificial impervious area have been well applied in urban precipitation researches (Su, Li et al. 2019). Most of these studies focused on individual UAs such as Beijing, Shanghai and the Pearl River Delta. There are also a few studies that give an overall landscape of the urbanization impact on climate at the national scale in China (Gu, Zhang et al. 2019, Lin, Gao et al. 2020). Therefore, it is very interesting to study the variation characteristics of the precipitation in the UAs within a unique climate zone.

The Loess Plateau (LP), located over the central-northern part of China and covering seven provinces and the middle reaches of the Yellow River, belongs to the wet-arid transition area and hence is sensitive to climate change. In recent decades, it has suffered severe water and soil losses and ecological environment changes, with decreasing trends of precipitation extreme in the Fen-Wei River valley and increasing trends of rainfall intensity and frequency in the northwestern LP, which exert negative effects on the social and economic developments (Zhao, Li et al. 2017, Zhang, Gao et al. 2020). Meanwhile, the LP has experienced drastically rapid urbanization in the last 20 years, and six typical UAs (Taiyuan, Xi'an, Hohhot, Yinchuan, Xining-Lanzhou and Luoyang) home to 70 percent of the LP population play an important role in the economic development and the ecological security(MA BB 2019). Precipitation over the LP is primarily affected by the complex terrain, the land-atmosphere interaction and the monsoon. During July to September, the East Asian summer monsoon has a dominant effect on the LP at a spatial scale far beyond the urban areas, which may overwhelm the local urban impacts. However, during April–June, the rainfall is much weaker and thus local urban effects may be more evident.

In this study, we present the first analysis of the changes of urban extreme precipitation over the LP in different climate zones based on a set of high-resolution gridded precipitation data. We also evaluate the contributions of climate change and urbanization to the urban precipitation across several UAs over the LP during different periods by using an effective attribution method.

The paper is structured as follows. Section 2 introduces the study area, the data, the definition of extreme climate events and the methods used in the study. Section 3 presents and discusses the analysis results. Conclusions are made in Section 4.

## 2. Data and Methods

### 2.1. Study area

The LP covers 62.4×104 km$^2$ (34–45°5'N, 101–114°33'N) and is located in the upper and middle reaches of the Yellow River in the central-northern part of China. The LP is surrounded by complicated mountain conditions, with the Yin Mountain in the north, the Qinling Mountain in the south, the Riyue Mountain in the west and the Taihang Mountain in the east. The terrain over the LP gradually declines from northwest to southeast, with a unique topography composed of abysses, ridges, gullies and hills. The LP lies in the continental monsoon climate zone, spanning 750 km from north to south and 1000 km from east to west, so the LP exhibits various climate characteristics (Zhang, Wu et al. 2014, Liu, Wang et al. 2016, Zhao, Zhai et al. 2017). The LP covers a wide temperature gradient decreasing from south to north and a large precipitation gradient decreasing from southeast to northwest.

### 2.2. Data

#### 2.2.1. China meteorological forcing dataset

The China Meteorological Forcing Dataset (CMFD) is a gridded near-surface meteorological dataset with high spatio-temporal resolution, which was developed by the hydrometeorological research group of the Institute of Tibetan Plateau Research of the Chinese Academy of Sciences. (Yang, He et al. 2010, Yingying, Chen et al. 2011). The dataset was obtained through fusion of remote sensing products, reanalysis dataset and in-situ observation data at weather stations. Its record starts from January 1979 and keeps extending (currently up to December 2018) with a temporal resolution of three hours and a spatial resolution of 0.1°. Seven near-surface meteorological elements are provided in the CMFD, including 2-m air temperature, surface pressure, specific humidity, 10-m wind speed, downward shortwave radiation, downward longwave radiation and precipitation rate.

#### 2.2.2. Global artificial impervious areas

Artificial impervious areas are predominant indicators of human settlements. Timely, accurate and frequent information on the artificial impervious areas is critical for understanding the urbanization process and the land use/cover change, as well as their impacts on the environment and the biodiversity. Based on the full archive of the 30-m resolution Landsat images on the Google Earth Engine platform, the annual global artificial impervious areas (GAIA) are mapped from 1985 to 2018 (Gong, Li et al. 2020). With the ancillary datasets, including the nighttime light data and the Sentinel-1 Synthetic Aperture Radar data, the performance of our previously developed algorithm is improved in arid areas. The GAIA dataset can be freely downloaded from http://data.ess.tsinghua.edu.cn.

The GAIA data with a spatial resolution of 30 m from 2000 to 2018 are used in this study to investigate the urbanization development over the LP during this period (He, Yang et al. 2020). According to the GAIA data in 2018 and 2000, there are six UAs over the LP, including Xi'an, Taiyuan, Luoyang, Hohhot, Yinchuan and Xining-Lanzhou (Fig. 1). The artificial impervious area in Xi'an, Taiyuan, Luoyang and Hohhot reached 1400 km$^2$,1700 km$^2$, 1000 km$^2$ and 1000 km$^2$ in 2018, which is 2 times, 2 times,1.5 times and 1.5 timesthat in 2000, respectively (Fig. 2). Due to the relatively slow economic development, the artificial impervious area in Yinchuan, Xining and Lanzhou only increased by 100–200 km$^2$ in 2018 compared to 2000.

#### 2.2.3. $PM_{2.5}$ hindcast database

The $PM_{2.5}$ hindcast database (PHD) provides the $PM_{2.5}$ estimation across China from 2000 to 2017. By using a machine learning approach, the PHD assembles datasets from multiple sources, including the moderate-resolution imaging spectroradiometer satellite measurements of aerosol, the Community Multiscale Air Quality model outputs based on the historical multi-resolution emission inventory for China and many other variables. It hindcasts the daily $PM_{2.5}$ concentrations from 2000 to 2017 in China. The PHD is developed and maintained by a team from Tsinghua University, Beijing, China (Xue, Zheng et al. 2019).

## 2.3. Methods

### 2.3.1. Trend detection

We analyze and discuss the extreme precipitation over the LP during the period from 1979 to 2018 by using the Mann-Kendall test and the Sen's slope estimator (Hamed 1998). The Mann-Kendall test is used to detect the significance of the change trend at each grid point. In this study, there are 13,500 grid points over the LP in the CMFD to be tested. At the 0.05 significance level, it will yield 675 (13,500 $\times$ 0.05) grid points where the significance cannot be determined, which is too high to be acceptable. Benjamini and Hochberg (1995) proposed the false discovery rate (FDR) procedure to apply the multiple Mann-Kendall tests to adjust the significance level and control the proportion of falsely rejected null hypotheses relative to the total number of rejected hypotheses.

The Sen's slope is applied to estimate the linear trend during 1979 to 2018 for each grid point (Sen and Kumar 1968). A positive slope value indicates an increasing or upward trend in the time series, while a negative value reveals a decreasing or downward trend. Similarly, zero indicates no trend.

### 2.3.2. Estimation of urbanization and climate change contribution

In this study, we evaluate the contribution of climate change and urbanization based on the "trajectory" method (Feng, H. et al. 2014, Feng and Huihui 2016). At local scales, climate change and urbanization jointly influence the precipitation trends at some certain grids. Their potential contributions at a certain UA can be calculated as follows.

$UE = R_u\text{-}R_r$ , (1)

$UC = S_{sub}\ x(R_u\ \text{-}R_r)/R_u x100\%$ , (2)

$CC = (R_r/R_u)x100\%$ , (3)

where $R_u$ and $R_r$ are the precipitation trends in urban and rural areas, respectively. The urbanization effect (UE) is defined as the trend difference between the urban and the rural series in Eq. 1. $S_{sub}$ is the proportion of urban grids to total grids. If the rural and the urban grids have the same number in the contribution analysis at regional scale, the parameter $S_{sub}$ can still be remained for the sake of equation generality. The relative urbanization contribution (UC) in percentage is defined as the fraction of the overall trends of the extreme precipitation events attributed to the UE in Eq. 2. The relative climate change contribution (CC) is defined as the ratio of the precipitation trend in the rural areas to that in the urban areas in Eq. 3 (Gu, Zhang et al. 2019).

### 2.3.4. Extreme precipitation index

We adopt the precipitation data from April 1 to July 1 in this study, excluding the persistent heavy precipitation caused by summer monsoon. Four extreme precipitation indices are selected to represent the intensity of presummer precipitation over the LP based on the gridded data in the CMFD. The four indices include the maximum daily precipitation ($R_{max}$), the very wet day precipitation ($R_{95p}$) which is the total precipitation when daily precipitation $> 95^{th}$ percentile mean daily precipitation, the extremely heavy precipitation ($R_{>10mm}$) which is the total precipitation when daily precipitation >10 mm and the number of light rain days ($R_{<10mm}$) which is the count of days with daily precipitation < 10 mm during the presummer season.

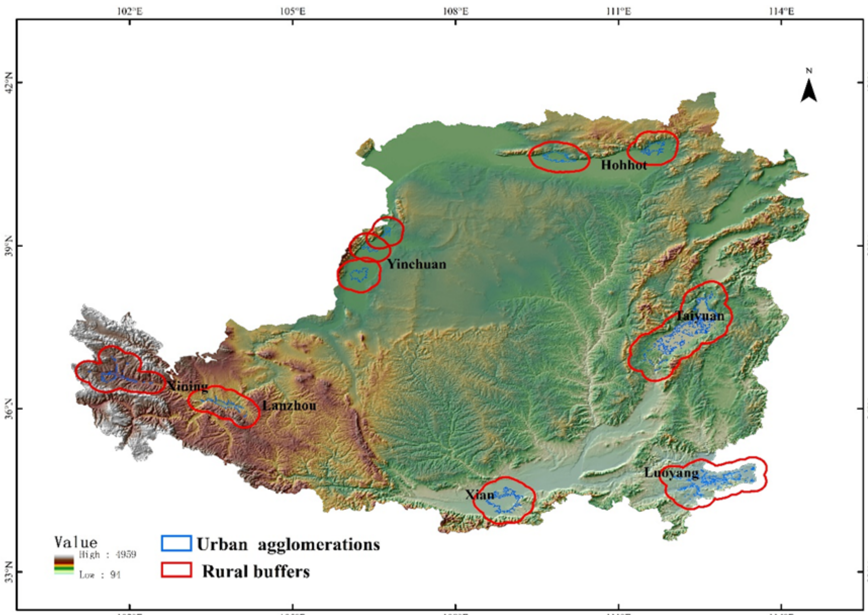


FIG. 1. Terrain height and urban agglomerations over the Loess Plateau.

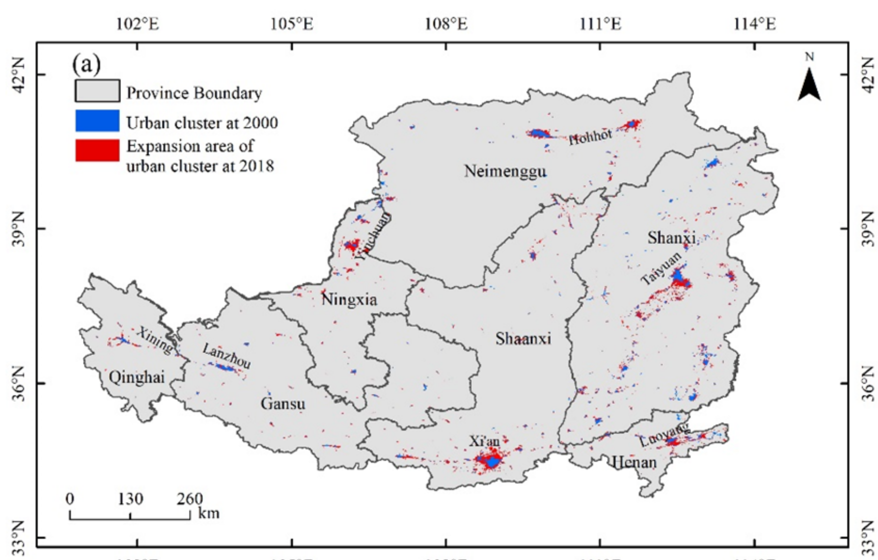

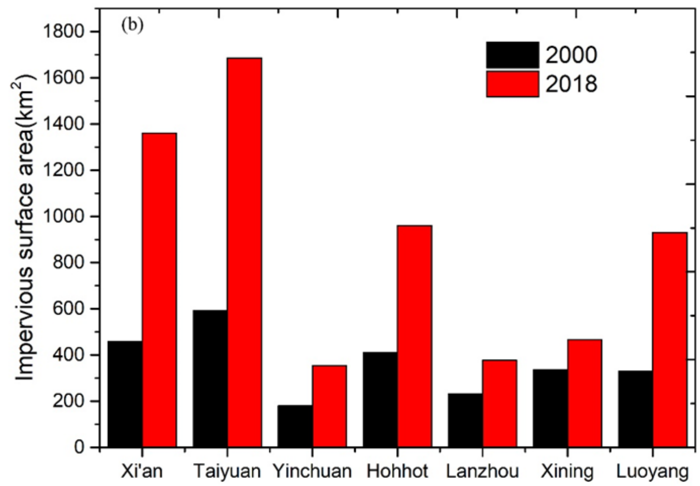


FIG. 2. Spatial distribution (a) and temporal variation (b) of the urban agglomeration area in 2000 and 2018 over the Loess Plateau.

## 3. Results and discussion

### 3.1. Spatial distributions of presummer precipitation trends

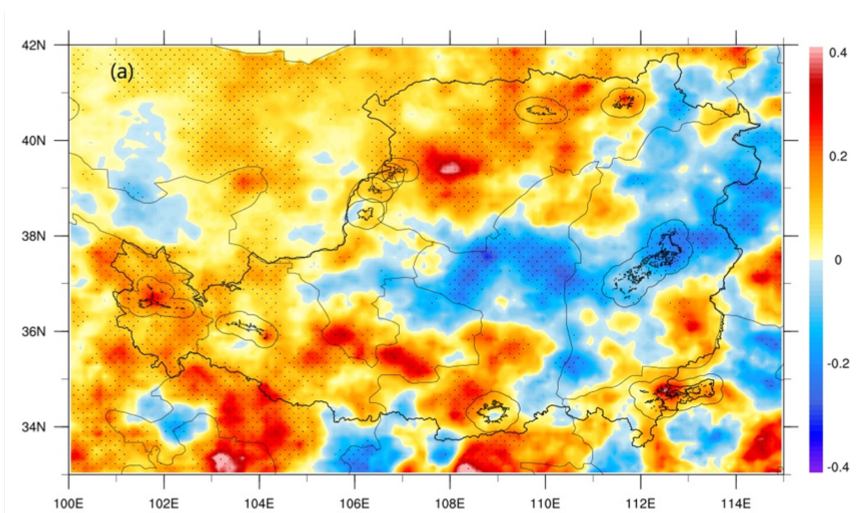

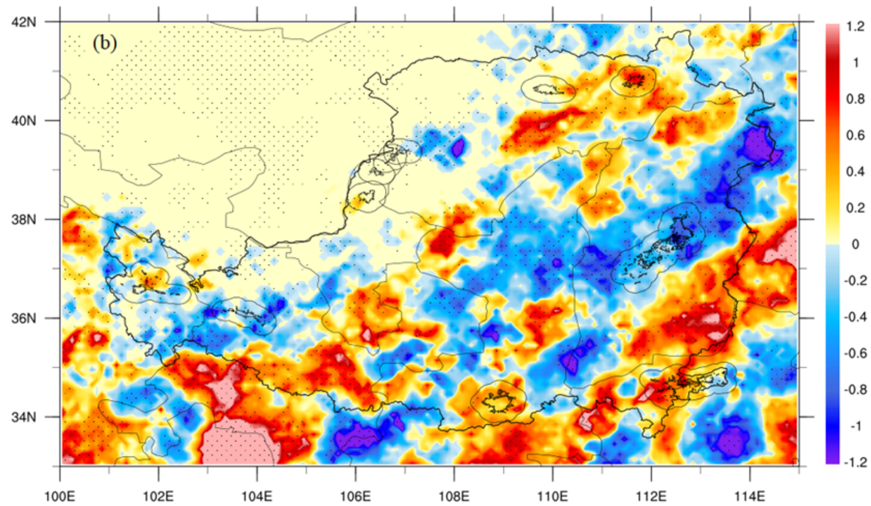
(b)
42N
40N
38N
36N
34N
100E
102E
104E
106E
108E
110E
112E
114E
1.2
1
0.8
0.6
0.4
0.2
0
-0.2
-0.4
-0.6
-0.8
-1
-1.2

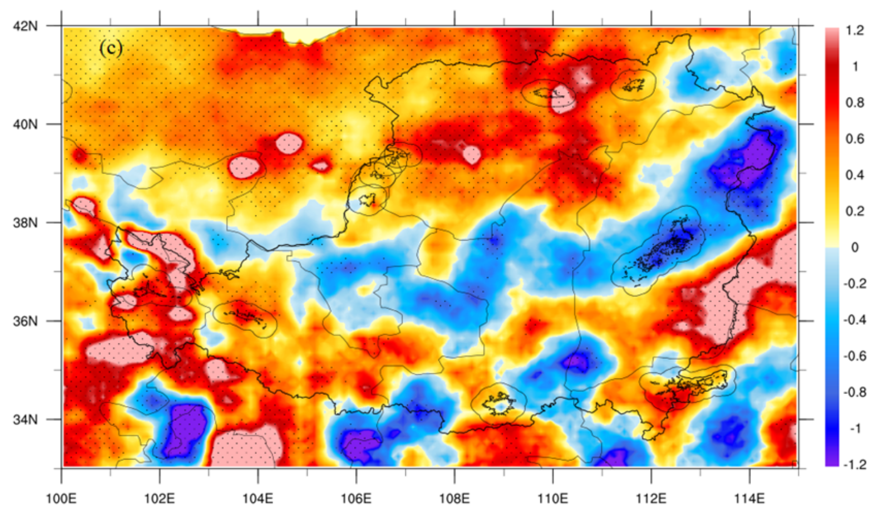
(c)
42N
40N
38N
36N
34N
100E
102E
104E
106E
108E
110E
112E
114E
1.2
1
0.8
0.6
0.4
0.2
0
-0.2
-0.4
-0.6
-0.8
-1
-1.2

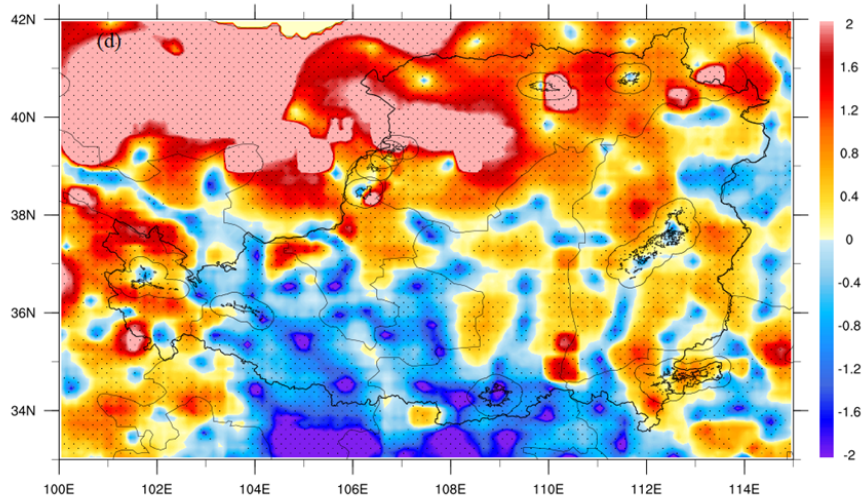


FIG. 3. Spatial distributions of the linear trends of (a) $R_{max}$, (b) $R_{>10mm}$, (c) $R_{95p}$ and (d) $R_{<10mm}$ over the Loess Plateau during the presummer season from 1979 to 2018.

The FDR-adjusted Mann-Kendall test is applied to detect the significance of the trend of the four presummer precipitation indices during 1979–2018 at each grid point over the LP. The black dots indicate the grid points with the trend passing the significance test at 90% confidence level. In general, the extreme precipitation increases in the northwest and decreases in the southeast of the LP (Fig. 3), which is basically consistent with the precvious studies (Zhao, Zhai et al. 2017, Zhao, Li et al. 2017). However, significant differences are found among the six UAs. Xi'an, Taiyuan and Luoyang are located in the Fenhe and Weihe River Basin in the southeastern LP, with the fastest urbanization development over the LP (Fig. 2). Under the climate background with decreasing precipitation, the extreme precipitation decreases more severely in Taiyuan UA and the rural areas. The rates of $R_{max}$, $R_{>10mm}$ and $R_{95p}$ in Taiyuan UA are 0.2 mm·year $^{-1}$, 0.4-0.6 mm*year$^{-1}$ and 0.4-0.5 mm*year $^{-1}$, respectively, which are lower than those in the rural areas. The most significant effect of urbanization is found in Taiyuan UA (Fig. 3c), where the decrease rates of $R_{95p}$ in the urban and the rural areas presents clearly different distributions. In obvious contrast with Taiyuan, Luoyang is under a climate background with increasing precipitation, and an obvious center with increasing extreme precipitation is found in Luoyang UA. The increase rates of $R_{max}$, $R_{>10mm}$ and $R_{95p}$ in Luoyang UA are 0.3 mm*year $^{-1}$, 0.7 mm*year $^{-1}$ and 0.9 mm*year $^{-1}$, respectively, which are higher than those in its rural region. Xi'an is different from the two above UAs. Xi'an UA is in a wet environment, but a dry core is formed in the UA center due to the urbanization effect, which is obviously reflected in the distribution of $R_{max}$ and $R_{95p}$ (Figs. 3a and 3c). The extreme precipitation rate decreases by 0.4-0.6 mm*year$^{-1}$ in the center of Xi'an UA compared with that in the rural areas. Hohhot and Xining are two UAs in the northern and western parts of the LP, respectively, where the precipitation has increased significantly in recent years. In the past two decades, the urbanization of Xining has been relatively slow, but it is particularly sensitive to the urbanization as a plateau city. The extreme precipitation in Xining UA is more concentrated in the center, especially for $R_{max}$ and $R_{>10mm}$. Hohhot has witnessed rapid urbanization in recent years, and its extreme precipitation characteristics are similar to those of Xining. The trend distribution of the number of light rain days is one of the most sensitive indicators for the urbanization effect. Different from the trend of extreme precipitation, the number of light rain days in the five UAs consistently decreases except for Luoyang, which corresponds to the change in the artificial impervious area (Figs. 2a and 4d).

The trends of extreme precipitation in Taiyuan, Luoyang, Hohhot and Xining UAs almost pass the significance test at 90% confidence level, while that in Xi'an does not pass the significance test, with opposite trend in the urban and the rural areas. The above analysis shows that the urbanization plays an accelerator role in the urban climate evolution, and the urban precipitation has become more intense and sensitive than that in the rural areas.

### 3.2. Trends variation of presummer precipitation in UAs

In order to further investigate the effect and contribution of climate change and urbanization on the presummer precipitation in different periods, we divide the five UAs into urban and rural areas separately according to the map of artificial impervious area cover. The UA area is covered by the artificial impermeable area, and the rural areas are mapped by using a buffer method. A buffer zone of 20 kilometers around the urban area is defined as the rural buffers (Fig. 1). The precipitation differences between the urban and the rural areas are calculated and compared in this section. The 30-m resolution land cover map is regridded into a 0.1deg GAIA map according to the spatial resolution of the CMFD dataset. For each grid of the new GAIA map, if the area of the original urban grids accounts for over 50% of its total area, it is defined as an urban grid; otherwise, it is defined as a rural grid. The precipitation indices are then spatially averaged over the urban and the rural grids separately, and the trend of each index is calculated based on the spatial mean during 1979–2018.

The analysis of section 3.1 reveals that the urbanization plays a role in amplifying the local climate change. Although the climate change is the main contributor to the urban precipitation trend, the effect of urbanization has been gradually identified in recent years. We apply the Student's t-test to detect the change point of the precipitation over the LP and divide the study periods into two stages. Most of the extreme precipitation indices in the five UAs demonstrate a sudden change point in the middle or late 1990s (Table 1). This is in accord with the previous studies indicating an obvious inter-decadal variation of the precipitation over the LP, with the significant turning point in the middle and late 1990s. During this period, the UAs had been growing more rapidly. Therefore, it is inferred that the climate change plays a primary role in the first stage of the precipitation series, and the urbanization effect gradually emerges in the second stage.

Figures 4 to 7 and Table 1 display the evolution of $R_{max}$, $R_{10mm}$, $R_{95p}$ and the light rain days in the five UAs and their rural areas. In the first stage, the extreme precipitation exhibits consistent trends in the urban and the rural areas of the five UAs (Fig. 4 and Table 1). However, the discrepancies between the urban and the rural widen in the second stage. The $R_{max}$, $R_{10mm}$ and $R_{95p}$ keep growing slowly in both the urban and the rural areas of Xi'an before 2001, however, the trends of extreme precipitation become discrepant between the urban and the rural areas after 2001, with increase in the urban areas and decrease in the rural areas. The $R_{max}$, $R_{10mm}$ and $R_{95p}$ in the urban and the rural areas of Taiyuan maintain a decreasing trend, which becomes steeper in the urban areas than in the rural areas in the second stage. For example, the trends of $R_{95p}$ in the urban and the rural areas of Taiyuan after 2001 are -1.09 mm*year $^{-1}$and -0.06 mm*year $^{-1}$, respectively (Table 2). The $R_{max}$, $R_{10mm}$ and $R_{95p}$ in Xining, Hohhot and Luoyang show a consistent increase trend in both the urban and the rural areas. In the second stage, the increase rates in the urban areas get greater than that in the rural areas, all of which are significant at a 0.10 significance level (Table 2). The linear trends of the number of light rain days in the five UAs show similar characteristics in the two stages, but the variation is significant. In the second stage, the number of light rain days in the rural areas of Hohhot, Taiyuan and Xining increases more significantly than that in the urban areas, on the contrary, that in the urban areas of Xi'an decreases much more than that in the rural areas. As a result, the number of light rain days increases less in the urban areas than in the rural areas. The above analyses illustrate that the climate change is the dominant factor for the urban precipitation in the first stage, but the urbanization effect is further revealed in the second stage.

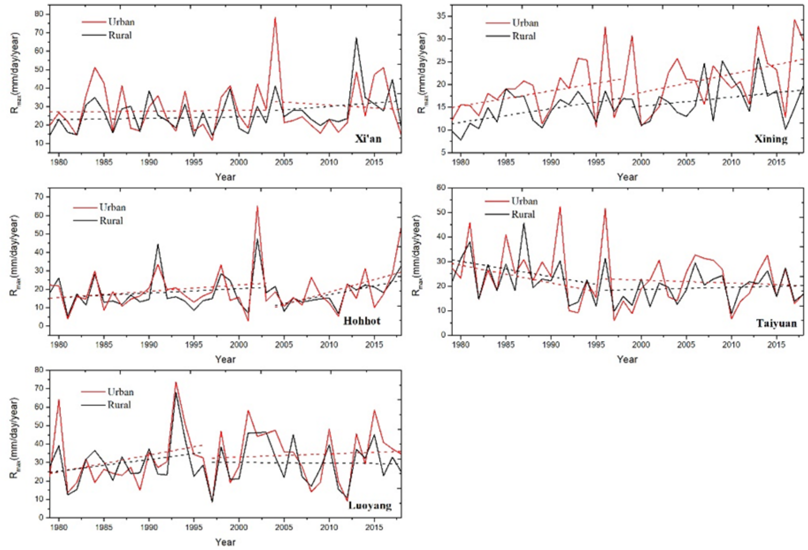


FIG. 4. Trend variation of presummer $R_{max}$ in the urban (red lines) and the rural (black lines) areas of the five UAs over the Loess Plateau during 1979–2018.

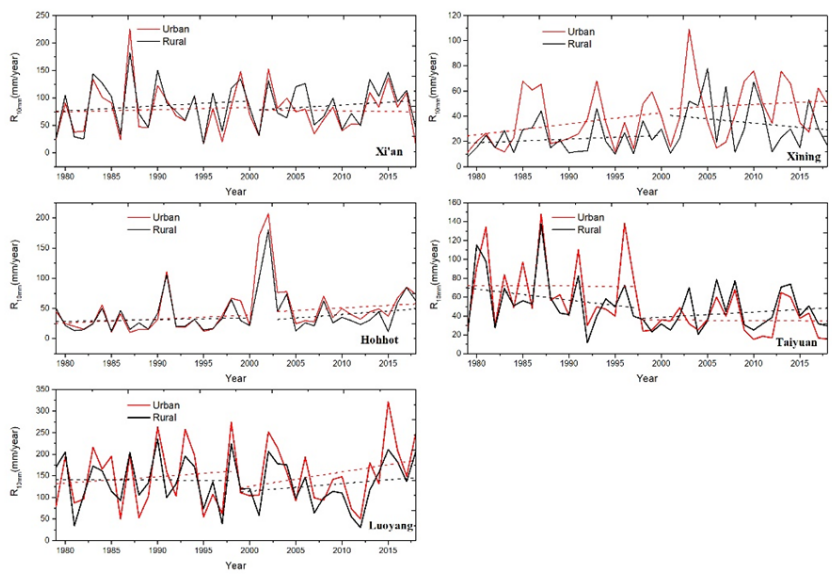


FIG. 5. The same as Fig. 4, but for $R_{10mm}$.

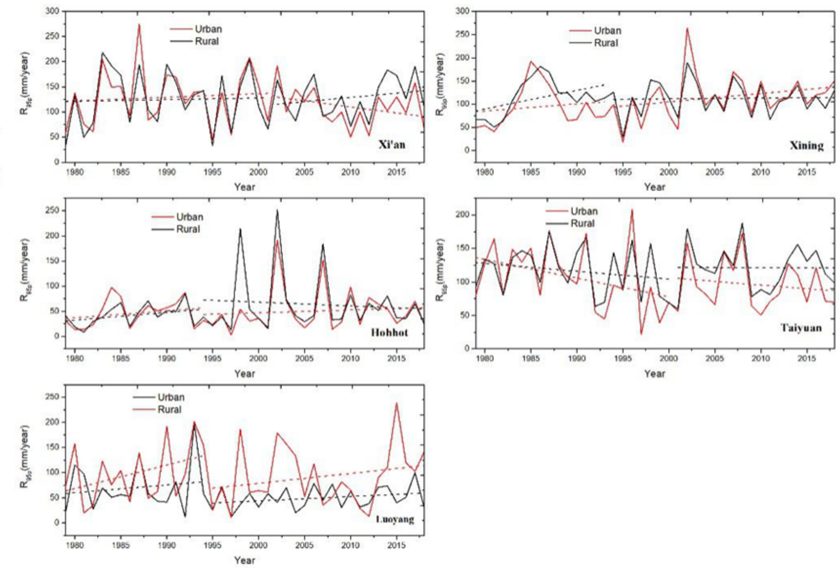


FIG. 6. The same as Fig. 4, but for $R_{95p}$.

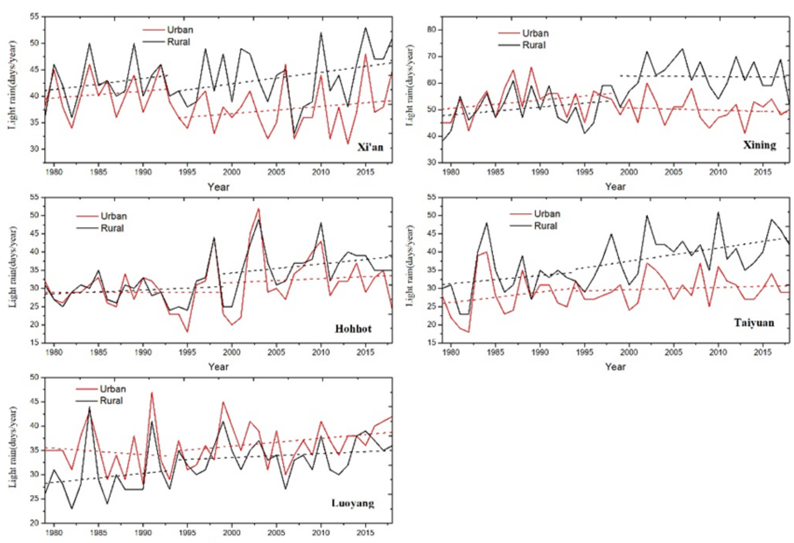


FIG. 7. The same as Fig. 4, but for light rain days.

To further quantify the contribution of climate change and urbanization to the precipitation, Table 2 shows the changes of the relative contributions in the two stages in the five UAs of the LP. Spatially, the urbanization tends to exert negative impacts on the extreme precipitation indices in the basin areas (such as Taiyuan and Xi'an) except for Luoyang in the southeastern LP, while positive urbanization effects are mainly found in the UAs located in the north and the west of the LP (including Hohhot and Xining). It is also found that the effect and contribution of urbanization are not only dependent on the study period, but also strongly correlated to the trend of th extreme precipitation index. In the first stage, the effect and contribution of urbanization on the urban precipitation are relatively weak, and the climate change is the dominant factor. In the second stage, the effect and contribution of urbanization have increased dramatically in most UAs, while the contribution of climate change is much weaker than that in the first stage. Among these extreme precipitation indices, the $R_{10mm}$ and the $R_{95p}$ in Luoyang and the $R_{10mm}$ in Hohhot demonstrate little differences of urban effect between the two stages, indicating that the urbanization does not always have a strong effect on all the extreme precipitation indices. In addition, the urbanization tends to augment the trends of precipitation caused by the climate change in all the five UAs. (For example, the urban areas of Taiyuan and Xi'an have become drier and Hohhot and Xining become wetter than their surrounding rural areas. The wetting trend in northwestern LP and the drying trend in southeastern LP were only attributed to the climate change in the previous researches. The results in this study demonstrate that the urbanization also plays an important role in the extreme precipitation change in the recent two decades.

TABLE 1. Mean trend of presummer precipitation from 1979 to 2018.

| city | $\mathbf{R_{max}}$ | $\mathbf{R_{max}}$ | $\mathbf{R_{max}}$ | $\mathbf{R_{10mm}}$ | $\mathbf{R_{10mm}}$ | $\mathbf{R_{10mm}}$ | $\mathbf{R_{95p}}$ | $\mathbf{R_{95p}}$ |
|---|---|---|---|---|---|---|---|---|
| | mm/day/year<br>Change point | mm/day/year<br>urban | mm/day/year<br>rural | mm/year<br>Change point | mm/year<br>urban | mm/year<br>rural | mm/year<br>Change point | mm/y<br>urban |
| **Xi'an** | 2003 | | | 2000 | | | 2001 | |
| | 1979-2003 | 0.04 | 0.06 | 1979-2000 | 0.4 | 0.9* | 1979-2001 | 0.7* |
| | 2004-2018 | -0.3* | 0.38* | 2001-2018 | -0.21 | 0.99* | 2002-2018 | -2.4* |
| **Xining** | 1998 | | | 2000 | | | 1994 | |
| | 1979-1998 | 0.33 | 0.29 | 1979-2000 | 0.8* | 0.28 | 1979-1994 | 1.53* |
| | 1999-2018 | 0.40* | 0.19 | 2001-2018 | 0.36 | -0.67* | 1995-2018 | 1.79* |
| **Hohhot** | 2003 | | | 2002 | | | 1994 | |
| | 1979-2003 | 0.34 | 0.24 | 1979-2001 | 0.65* | 0.29 | 1979-1994 | 1.43* |
| | 2004-2018 | 1.35* | 0.95* | 2003-2018 | 0.85* | 0.67* | 1995-2018 | 0.54* |
| **Taiyuan** | 1995 | | | 1997 | | | 2001 | |
| | 1979-1995 | -0.71* | -0.62* | 1979-1997 | -0.01 | -1.16* | 1979-2001 | -2.77* |
| | 1996-2018 | -0.12 | 0.08 | 1998-2018 | -0.05 | 0.54* | 2002-2018 | -1.09* |
| **Luoyang** | 1996 | | | 1999 | | | 1994 | |
| | 1979-1996 | 0.90* | 0.63* | 1979-1999 | 1.5* | -0.08 | 1979-1994 | 4.67* |
| | 1997-2018 | 0.17 | -0.06 | 2000-2018 | 3.34* | 1.75* | 1995-2018 | 1.96* |

*The trend is significant at the 0.10 significance.

TABLE 2. Mean trends of urbanization effect (unit: per year), relative urbanization and climate change contribution (unit: in the two stages.

| **City** | **Stage** | $\mathbf{R_{max}}$ | $\mathbf{R_{max}}$ | $\mathbf{R_{max}}$ | $\mathbf{R_{10mm}}$ | $\mathbf{R_{10mm}}$ | $\mathbf{R_{10mm}}$ | $\mathbf{R_{95p}}$ | $\mathbf{R_{95p}}$ | $\mathbf{R_{95p}}$ | **Light Rain** | **Light** |
|---|---|---|---|---|---|---|---|---|---|---|---|---|
| | | **UE** | **UC** | **CC** | **UE** | **UC** | **CC** | **UE** | **UC** | **CC** | **UE** | **UC** |
| Xi'an | I | -0.02 | -50.0 | 100 | -0.52 | -49.5 | 100 | 0.25 | 35.7 | 100 | -0.08 | -66.7 |
| | **II** | **-0.71** | **-92.5** | **-100** | **-1.21** | **-81.8** | **-100** | **-4.07** | **-58.9** | **-100** | **-0.07** | **-57.2** |
| Xining | I | 0.04 | 12.1 | 87.8 | 0.51 | 62.5 | 35.0 | -2.31 | -42.8 | 100 | 0.02 | 6.4 |
| | **II** | **0.20** | **50.0** | **42.5** | **1.01** | **95.6** | **-100** | **1.52** | **84.9** | **8.3** | **-0.06** | **-75.0** |
| Hohhot | I | 0.10 | 29.4 | 70.5 | 0.37 | 56.9 | 44.4 | -0.08 | -5.6 | 100 | 0.09 | -90.0 |
| | **II** | **0.42** | **31.1** | **70.3** | **0.14** | **17.8** | **78.8** | **1.33** | **41.3** | **-100** | **-0.15** | **-95.5** |
| Taiyuan | I | -0.08 | -12.7 | 87.3 | -1.1 | -10.2 | 100 | -1.42 | 52.5 | 41.8 | -0.06 | -21.4 |
| | II | **-0.21** | **-57.1** | **-66.7** | **-0.6** | **-90.0** | **-100** | **-1.01** | **92.6** | **5.5** | **-0.23** | **-47.8** |
| Luoyang | I | 0.31 | 33.3 | 70.0 | 1.57 | 95 | -5.3 | 3.12 | 66.8 | 32.9 | -0.31 | -41.9 |

| City | Stage | $R_{max}$ | $R_{max}$ | $R_{max}$ | $R_{10mm}$ | $R_{10mm}$ | $R_{10mm}$ | $R_{95p}$ | $R_{95p}$ | $R_{95p}$ | Light Rain | Light |
|---|---|---|---|---|---|---|---|---|---|---|---|---|
| | II | **0.23** | **73.2** | **35.2** | **1.63** | **48.8** | **52.3** | **1.11** | **56.6** | **43.8** | **0.07** | **46.7** |

### 3.3. Urbanization effect on the presummer precipitation over the Loess Plateau

The previous analyses suggested that the changes in large-scale atmospheric circulations are likely the main cause of the variation in extreme precipitation patterns. However, the significant discrepancies between the trends in the urban and the rural areas indicate a remarkable effect of urbanization on the variability of extreme precipitation over the LP, especially in the last 20 years. The urbanization causes many climatic problems, such as the increase of urban surface temperature, the decrease of wind speed and the increase of aerosols. However, the physical process of the urbanization effect on the extreme precipitation is quite complicated. In this section, we only preliminarily discuss the possible effects of temperature and aerosols on the urban precipitation over the LP.

The UHI effect may be one factor influencing the presummer precipitation over the LP. Except for the Xining UA with unsignificant increase of surface air temperature, all the other UAs exhibit significant UHI characteristics, with the mean trend of surface temperature in the urban areas 0.05–0.07°C·year$^{-1}$ higher than that in the rural areas during 1979–2018 (Fig. 8). The previous studies showed that urbanization has different impacts on urban precipitation in wet and dry climate backgrounds (Luo and Lau 2019, Yang 2020). The warmer surface in the urban core areas induces stronger potential evapotranspiration by exponentially increasing the saturated water vapor pressure and aggravating the water vapor deficit. If the atmospheric water is scarce, the urbanization further intensifies the drying trend over the urban core areas compared with the surrounding rural areas, such as Xi'an and Taiyuan. If the atmospheric water is abundant, the heat source in the urban areas induces vertical flows and enhances convective motions, leading to more convective precipitation in the urban areas than in the rural areas, such as Luoyang and Hohhot (Yan, Chan et al. 2020).

Another major feature is the increasing aerosol emissions associated with urbanization. In this study, $PM_{2.5}$ is taken as a representative to reflect the aerosol distribution in the UAs over the LP (Fig. 9). Many studies have indicated that aerosols may inhibit or promote the precipitation with different intensity (Qian Duan 2008, Ma, Huo et al. 2017, Fults, Massmann et al. 2019, Berhane and Bu 2021). For instance, aerosols have obvious inhibitory effect on the light rain in general. With sufficient water vapor, more aerosol particles will lead more condensation nuclei to be formed (aerosol microphysical effect), which further increases the extreme precipitation combined with the UHI effect. The urban precipitation characteristics in Luoyang, Hohhot and Xining UAs can be explained in this way. However, in the long run, the increase of aerosol is not conducive to the precipitation formation. Aerosols weaken the radiation reaching the ground, leading to a stable low-level atmosphere, which is unfavorable for the ascending motion and thus reduces the occurrence frequency of precipitation. When the water vapor transport weakens, the increase of aerosol makes the atmospheric stratification more stable, resulting in less precipitation frequency. Xi'an and Taiyuan UAs have experienced frequent serious air pollution incidents in recent years due to the impact of basin topography and urbanization. The significant decrease of precipitation in the two UAs should be closely related to the increase of aerosol in recent years. Therefore, the urbanization influence on precipitation is actually the result of the competition among the thermal forcing of UHI, the aerosol radiation effect and the aerosol microphysical effect.

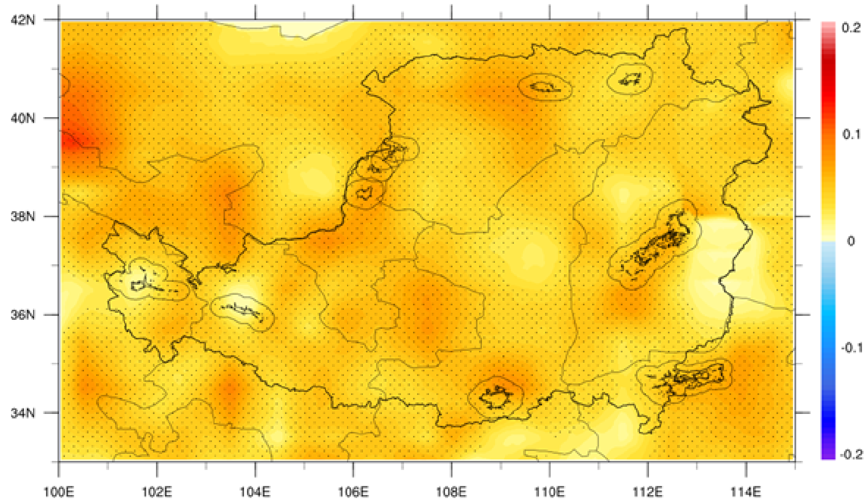


FIG. 8. Spatial distribution of the linear trends of mean temperature over the Loess Plateau during the presummer season from 1979 to 2018.

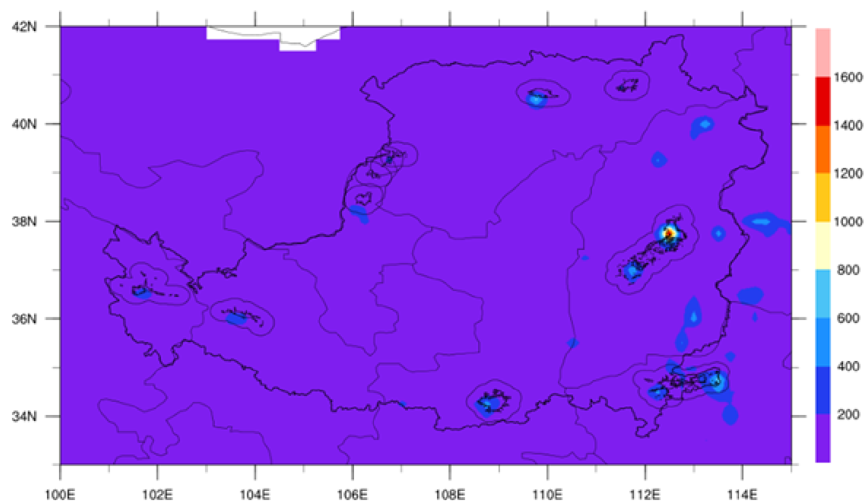


FIG. 9. Spatial distribution of the monthly mean PM2.5 over the Loess Plateau during the presummer season from 2000 to 2017.

## 4. Conclusion and discussion

The variation patterns of the extreme precipitation and the contributions of climate change and urbanization in the UAs over the LP from 1979 to 2018 are analyzed in this study. The results reveal that the precipitation intensity during the presummer season has decreased in the southeastern LP and increased in the northwestern LP, and the variation trends are much more significant in the urban areas than in the rural areas. Specifically, the urbanization can aggravate the decreasing trends of extreme precipitation in Taiyuan and Xi'an UAs while enhance the increasing trends in Luoyang, Hohhot and Xining UAs. The number of light rain days is very sensitive to the urbanization, which decreases in almost all the cities. Although Xining

UA has a lower level of urbanization compared to the other UAs over the LP, the urbanization effect is also detected in the wetting trend.

The results also display that the climate change is the dominant factor for the urban precipitation trends, but the urbanization exhibits different influences in different periods. In the first twenty years, the urbanization contribution in the urban precipitation is relatively weak, and the climate change is the primary factor. In the last twenty years, the urbanization contribution increases dramatically, while the contribution of climate change is much weaker than that in the first stage. The urbanization tends to exert negative impacts on the extreme precipitation indices in Xi'an and Taiyuan UAs and positive effects in Luoyang, Hohhot and Xining UAs. In addition, the stronger intensification of extreme precipitation in the urban areas may be closely connected with the faster increase of surface temperature and aerosol particles. To further examine the physical processes of the urbanization effect on the extreme events in the UAs over different geographical locations and under different climate backgrounds across the LP, the dynamic experiments based on the Weather Research and Forecasting model will be performed in our forthcoming studies.

The climate environment of the UAs over the LP is very sensitive and fragile. Due to the considerable trends of extreme precipitation caused by the climate change and amplified by the urbanization, urban disasters, such as urban water shortage and urban waterlogging, are expected to be further strengthened. Scientific urbanization planning and construction should attract attention to alleviate the urbanization consequences, particularly in large cities.

Reference:

Berhane, S. A. and L. Bu (2021). "Aerosol-Cloud Interaction with Summer Precipitation over Major Cities in Eritrea." *Remote Sensing* **13** (4): 21.

Daniel, M., et al. (2018). "Benefits of explicit urban parameterization in regional climate modeling to study climate and city interactions." *Climate Dynamics* **52** (5-6): 2745-2764.

Della-Marta, P. M., et al. (2007). "Doubled length of western European summer heat waves since 1880." *Journal of Geophysical Research* **112** (D15).

Drobinski, P., et al. (2016). "Scaling precipitation extremes with temperature in the Mediterranean: past climate assessment and projection in anthropogenic scenarios." *Climate Dynamics* **51** (3): 1237-1257.

Du, J., et al. (2019). "Urban Dry Island Effect Mitigated Urbanization Effect on Observed Warming in China." *Journal of Climate* **32** (18): 5705-5723.

Feng, et al. (2014). "Trajectory based detection of forest-change impacts on surface soil moisture at a basin scale [Poyang Lake Basin, China]." *JOURNAL OF HYDROLOGY -AMSTERDAM-* .

Feng and Huihui (2016). "Individual contributions of climate and vegetation change to soil moisture trends across multiple spatial scales." *Rep* **6** : 32782.

Fults, S. L., et al. (2019). "Wintertime aerosol measurements during the Chilean Coastal Orographic Precipitation Experiment." *Atmospheric Chemistry and Physics* **19** (19): 12377-12396.

Gong, P., et al. (2020). "Annual maps of global artificial impervious area (GAIA) between 1985 and 2018." *Remote Sensing of Environment* **236** .

Gu, X., et al. (2019). "Potential contributions of climate change and urbanization to precipitation trends across China at national, regional and local scales." *International Journal of Climatology* **39** (6): 2998-3012.

Hamed, K. H. (1998). "<a modefied mann-kendall trend test for autocorrelated data.pdf>." *Journal of Hydrology* .

Han, J.-Y., et al. (2014). "Urban impacts on precipitation." *Asia-Pacific Journal of Atmospheric Sciences* **50** (1): 17-30.

He, J., et al. (2020). "The first high-resolution meteorological forcing dataset for land process studies over China." *Sci Data* **7** (1): 25.

Liao, W., et al. (2018). "Stronger Contributions of Urbanization to Heat Wave Trends in Wet Climates." *Geophysical Research Letters* **45** (20).

Lin, L., et al. (2020). "Contribution of urbanization to the changes in extreme climate events in urban agglomerations across China." *Sci Total Environ* **744** : 140264.

Liu, Z., et al. (2016). "Spatiotemporal analysis of multiscalar drought characteristics across the Loess Plateau of China." *Journal of Hydrology* **534** : 281-299.

Luo, M. and N. C. Lau (2018). "Increasing Heat Stress in Urban Areas of Eastern China: Acceleration by Urbanization." *Geophysical Research Letters* **45** (23).

Luo, M. and N. C. Lau (2019). "Urban Expansion and Drying Climate in an Urban Agglomeration of East China." *Geophysical Research Letters* **46** (12): 6868-6877.

MA BB, Z. K. L. H. (2019). " Spatiotemporal differentiation and influence factors of vulnerability for urban "socio-economic" system in the Loess Plateau." *Journal of Shaanxi Normal University (Natural Science Edition)* **47** (4): 8.

Ma, H., et al. (2017). "Impact of Chinese Urbanization and Aerosol Emissions on the East Asian Summer Monsoon." *Journal of Climate* **30** (3): 1019-1039.

Ma, H., et al. (2018). "Unexpected large-scale atmospheric response to urbanization in East China." *Climate Dynamics* **52** (7-8): 4293-4303.

Paul, S., et al. (2018). "Increased Spatial Variability and Intensification of Extreme Monsoon Rainfall due to Urbanization." *Sci Rep* **8** (1): 3918.

Qian Duan, J. M. (2008). "The Impact of Aerosol on Regional Precipitation in North China." *science bulletin* **53(23)** .

Sen and P. Kumar (1968). "Estimates of the Regression Coefficient Based on Kendall's Tau." *Publications of the American Statistical Association* **63** (324): 1379-1389.

Su, L., et al. (2019). "Spatiotemporal Variation in Presummer Precipitation Over South China From 1979 to 2015 and Its Relationship With Urbanization." *Journal of Geophysical Research: Atmospheres* .

Wang, W., et al. (2007). "Climate Response to Rapid Urban Growth: Evidence of a Human-Induced Precipitation Deficit." *Journal of Climate* **20** (10): 2299-2306.

Xue, T., et al. (2019). "Spatiotemporal continuous estimates of PM2.5 concentrations in China, 2000–2016: A machine learning method with inputs from satellites, chemical transport model, and ground observations." *Environment International* **123** : 345-357.

Yan, M., et al. (2020). "Impacts of Urbanization on the Precipitation Characteristics in Guangdong Province, China." *Advances in Atmospheric Sciences* **37** (7): 696-706.

Yang, K., et al. (2010). "On downward shortwave and longwave radiations over high altitude regions: Observation and modeling in the Tibetan Plateau." *Agricultural & Forest Meteorology* **150** (1): 38-46.

Yang, Q. Z. J. H. Z. (2020). " Spatiotemporal characteristics of regional precipitation events in the Jing-Jin-Ji region during 1989–2018."

Yingying, et al. (2011). "Improving land surface temperature modeling for dry land of China." *Journal of Geophysical Research Atmospheres* .

Zhang, B., et al. (2014). "Spatiotemporal analysis of climate variability (1971-2010) in spring and summer on the Loess Plateau, China." *Hydrological Processes* **28** (4): 1689-1702.

Zhang, J., et al. (2020). "A universal multifractal approach to assessment of spatiotemporal extreme precipitation over the Loess Plateau of China." *Hydrology and Earth System Sciences***24** (2): 809-826.

Zhao, D. and J. Wu (2017). "Changes in urban-related precipitation in the summer over three city clusters in China." *Theoretical and Applied Climatology* **134** (1-2): 83-93.

Zhao, G., et al. (2017). "Variations in extreme precipitation on the Loess Plateau using a high-resolution dataset and their linkages with atmospheric circulation indices." *Theoretical and Applied Climatology* **133** (3-4): 1235-1247.

Zhao, X., et al. (2017). "Change of precipitation characteristics in the water-wind erosion crisscross region on the Loess Plateau, China, from 1958 to 2015." *Sci Rep* **7** (1): 8048.

### Hosted file

`table.docx` available at https://authorea.com/users/436835/articles/538884-contribution-of-climate-change-and-urbanization-to-the-variation-of-extreme-precipitation-in-the-urban-agglomerations-over-the-loess-plateau

### Hosted file

`figure.docx` available at https://authorea.com/users/436835/articles/538884-contribution-of-climate-change-and-urbanization-to-the-variation-of-extreme-precipitation-in-the-urban-agglomerations-over-the-loess-plateau